small method
www.small-methods.com

Polymer Coatings to Minimize Protein Adsorption in Solid-State Nanopores

Saurabh Awasthi, Pongsatorn Sriboonpeng, Cuifeng Ying, Jared Houghtaling, Ivan Shorubalko, Sanjin Marion, Sebastian James Davis, Laura Sola, Marcella Chiari, Aleksandra Radenovic, and Michael Mayer**

Nanopore-based resistive-pulse recordings represent a promising approach for single-molecule biophysics with applications ranging from rapid DNA and RNA sequencing to "fingerprinting" proteins. Based on advances in fabrication methods, solid-state nanopores are increasingly providing an alternative to proteinaceous nanopores from living organisms; their widespread adoption is, however, slowed by nonspecific interactions between biomolecules and pore walls, which can cause artifacts and pore clogging. Although efforts to minimize these interactions by tailoring surface chemistry using various physisorbed or chemisorbed coatings have made progress, a straightforward, robust, and effective coating method is needed to improve the robustness of nanopore recordings. Here, covalently attached nanopore surface coatings are prepared from three different polymers using a straightforward "dip and rinse" approach and compared to each other regarding their ability to minimize nonspecific interactions with proteins is compared. It is demonstrated that polymer coatings approach the performance of fluid lipid coatings with respect to minimizing these interactions. Moreover, these polymer coatings enable accurate estimates of the volumes and spheroidal shapes of freely translocating proteins; uncoated or inadequately coated solid-state pores do not have this capability. In addition, these polymer coatings impart physical and chemical stability and enable efficient and label-free characterization of single proteins without requiring harsh cleaning protocols between experiments.

1. Introduction

Nanopores enable the characterization of unlabeled biomolecules in their native state on a single-molecule level in aqueous solution.[1–4] Nanopore-based approaches for DNA and RNA sequencing with long read lengths have progressed to commercially available next-generation DNA sequencing technologies[5,6] in a portable format.[7] Broadly speaking, nanopores can be classified as biological,[8] solid-state,[9] or a combination of the two.[10] Biological nanopores include channel proteins such as the product of Curli specific gene G (CsgG) from *Escherichia coli*,[11] α-hemolysin (αHL) from *Staphylococcus aureus*,[12] *Mycobacterium smegmatis* porin A (MspA)[13] and *Aeromonas hydrophila* Aerolysin (AeL),[14] which spontaneously embed themselves in a lipid bilayer. These types of nanopores can be produced in large numbers by protein expression and purification, have well-characterized crystal structures, and have played a critical role in advancing the resistive pulse sensing technique.[15–17] It is, however, difficult to generate protein pores with diameters that exceed 4 nm. Another limitation is the need to reconstitute these protein pores into lipid or block copolymer membranes, which can be mechanically and chemically fragile.[18] Conversely, solid-state nanopores can be fabricated in various materials such as silicon nitride, silicon oxide, aluminum oxide, hafnium oxide, or graphene.[9,19] Their diameters and geometries can be tuned depending on user requirements, and they can be used repeatedly for experiments with considerable experimental flexibility (e.g., temperature, buffer conditions, presence of detergents or solvents, extreme pH values, applied potential differences, etc.).[20–22] Despite these attractive characteristics, solid-state nanopores suffer from at least three drawbacks. First, they usually interact nonspecifically with biomolecules, leading to resistive pulse artifacts such as attenuated rotation, translation and

Dr. S. Awasthi, P. Sriboonpeng, Dr. C. Ying, Dr. J. Houghtaling, Prof. M. Mayer
Adolphe Merkle Institute
University of Fribourg
Chemin des Verdiers 4, Fribourg CH-1700, Switzerland
E-mail: saurabh.awasthi@unifr.ch; michael.mayer@unifr.ch

The ORCID identification number(s) for the author(s) of this article can be found under https://doi.org/10.1002/smtd.202000177.

DOI: 10.1002/smtd.202000177

Dr. I. Shorubalko
Laboratory for Transport at Nanoscale Interfaces
Empa–Swiss Federal Laboratories for Materials Science and Technology
Überlandstrasse 129, Dübendorf CH-8600, Switzerland

Dr. S. Marion, S. J. Davis, Prof. A. Radenovic
Laboratory of Nanoscale Biology
Institute of Bioengineering
School of Engineering
EPFL
Lausanne 1015, Switzerland

Dr. L. Sola, Dr. M. Chiari
Istituto di Scienze e Tecnologie Chimiche (SCITEC)
CNR
Via Mario Bianco 9, Milano 20131, Italy

clogging.[23] Second, and often overlooked, nanopores in thin insulating windows (e.g., 20 nm thick SiN_x) often grow in diameter by slow etching in aqueous electrolyte. And third, materials best suited for nanoscale fabrication often present surface charges that can give rise to flicker noise, electroosmotic flow (EOF) and ion current rectification in the presence of electric fields.[24,25] Strategies now exist to overcome some of these limitations, including atomic layer deposition (ALD),[26] physisorption of surfactants,[27,28] polymer coatings,[29] silanization,[30,31] fluid lipid bilayer coatings[32–35] and various other surface modifications.[36–38] Emilsson et al. demonstrated that surface coating in the form of poly(ethylene glycol) brushes, can be used for gating solid-state nanopores.[39] Roman et al. made use of solid-state nanopore coated with poly(ethylene glycol (PEG) in reusable microfluidic devices to achieve more stability for detecting gold particles or spherical proteins compared to uncoated surfaces.[40,41] Nonetheless, the ideal coating for nanopores would minimize nonspecific interactions, reduce surface charge, and lower the electrical noise during recording. Moreover, this ideal coating would be straightforward to apply, would stabilize the diameter of coated pores for extended time in aqueous electrolyte and would make it possible to interrogate different analytes by simply rinsing the coated chips between experiments. Finally, this ideal coating would allow tuning the pore diameter and incorporating specific functional groups such that specific analytes could be captured and interrogated.[38]

In previous work, we coated solid-state nanopores with fluid lipid bilayers, which not only minimized nonspecific surface interactions between translocating molecules and the pore walls, but also made it possible to estimate physical parameters such as the ellipsoidal shape, volume, and dipole moment of single proteins.[32,35] Here, we compare alternative coatings based on covalently attached polymers as alternatives to lipid bilayer coatings with respect to their ability to minimize nonspecific interaction between protein and the pore wall. We coat solid-state nanopores in silicon nitride widows with one of three different polymers: i) poly(acrylamide)-g-(poly(2-methyl-2-oxazoline, 1,6-hexanediamine, 3-amino-propyldimethylsilanol) in short PAcrAm-g-PMOXA, ii) poly(acrylamide)-g-(PEG, 1,6-hexanediamine, 3-amino-propyldimethylsilanol) in short PAcrAm-g-PEG, and iii) a poly(dimethyl acrylamide) copolymer with glycidyl methacrylate in short copoly(DMA-GMA-MAPS). We confirm the presence of PAcrAm-g-PMOXA, PAcrAm-g-PEG on the nanopore chips using X-ray photoelectron spectroscopy (XPS). We also measure the thickness of these polymer coatings in the dry state using ellipsometry and estimate their thickness in the hydrated state by measuring the pore resistance in aqueous electrolyte before and after coating. We chose these polymers because Weydert et al. already demonstrated the stability and antifouling property of PAcrAm-g-PMOXA in comparison with the PLL-g-PEG, a commonly used antiadhesive polymer surface coating. They reported better stability and antifouling properties of PAcrAm-g-PMOXA in comparison to the PLL-g-PEG owing to the simultaneous physical and chemical attachment to the surface and antifouling property of PMOXA.[42] Moreover, Aramesh et al. recently used PAcrAm-g-PMOXA to coat solid-state nanopores that were located close to the tip of an atomic force microscope (AFM) and these nanopore tips made it possible to sense secreted molecules on the surface of living cells in culture without clogging.[43] Zilio et al. used copoly(DMA-GMA-MAPS), to minimize protein adsorption onto thermoplastics.[44] Here we show that nanopores coated with PAcrAm-g-PMOXA or PAcrAm-g-PEG perform almost as well as fluid lipid bilayer coatings with regard to their ability to minimize nonspecific interactions and to estimate the volume and the spheroidal shape of proteins from free translocations through these coated nanopores.

2. Results and Discussion

Figure 1a illustrates the basic experimental setup for a resistive pulse-based nanopore experiment: a thin insulating membrane with a single nanopore separates two compartments and a high-gain, low-noise amplifier applies a potential difference between them and monitors the ionic current through the nanopore. Translocations of macromolecules through the nanopore displace conducting electrolyte and produce characteristic resistive pulses (Figure 1b) that contain information about the physical properties of those biomolecules, including their volume and length-to-diameter ratio.[32,35,45–47] In order to prevent artifacts due to nonspecific adsorption of the biomolecules on the surface of the pore walls, we coated the pores with PAcrAm-g-PEG, PAcrAm-g-PMOXA, or P(DMA-GMA-MAPS) in a straightforward "dip and rinse" approach and compared their ability to minimize artifacts from protein adhesion. Figure 1c shows the different steps involved in the coating procedure. All three polymers contain silane groups to provide covalent attachment to surfaces that present silanol groups whereas PAcrAm-g-PEG and PAcrAm-g-PMOXA also contain positively charged amine groups to enable electrostatic interactions with negatively charged surfaces to attach the coatings to the surface. The PacrAm-g-PMOXA polymer also takes advantage of the poly(2-methyl-2-oxazoline) (PMOXA) moiety, which provides antifouling functionality to the polymer.[41] Zilio et al. reported that the "DMA interacts with the substrates through both hydrogen and hydrophobic bonds" in the case of the coatings from copoly(DMA-GMA-MAPS).[44]

Studies by XPS confirmed successful coating of nanopores in the case of PacrAm-g-PMOXA and PacrAm-g-PEG (see Figure S1 in the Supporting Information), ellipsometry determined a thickness of (1.1 ± 0.1) nm for the PacrAm-g-PMOXA coating and (2.5 ± 0.5) nm for the PAcrAm-g-PEG coating in the dry state and resistance measurements of the electrolyte-filled nanopore before and after coating indicated an apparent thickness of (2.0 ± 0.5) nm for the PacrAm-g-PMOXA coating and (5.0 ± 0.5) nm for the PAcrAm-g-PEG coating in the hydrated state. Serrano et al. reported the thickness of the polymeric film formed by poly(acrylamide)-g-(PEG, 1,6-hexanediamine, 3-amino-propyldimethylethoxysilane) on silicon dioxide surface to be about 2.5 nm at a PEG grafting density of more than 2.0 PEG chains per acrylate molecule.[48] We observed only a very small change in the nanopore resistance before and after coating with copoly(DMA-GMA-MAPS), suggesting a thin surface layer of polymer.

Because noise characteristics are critical for nanopore-based single-molecule studies, we compared the power spectral density (PSD) from ionic current recordings through nanopores before and after coating them with each polymer. **Figure 2** illustrates that the PAcrAm-g-PMOXA coating provided the best noise characteristics among the three polymer coatings; in fact, this

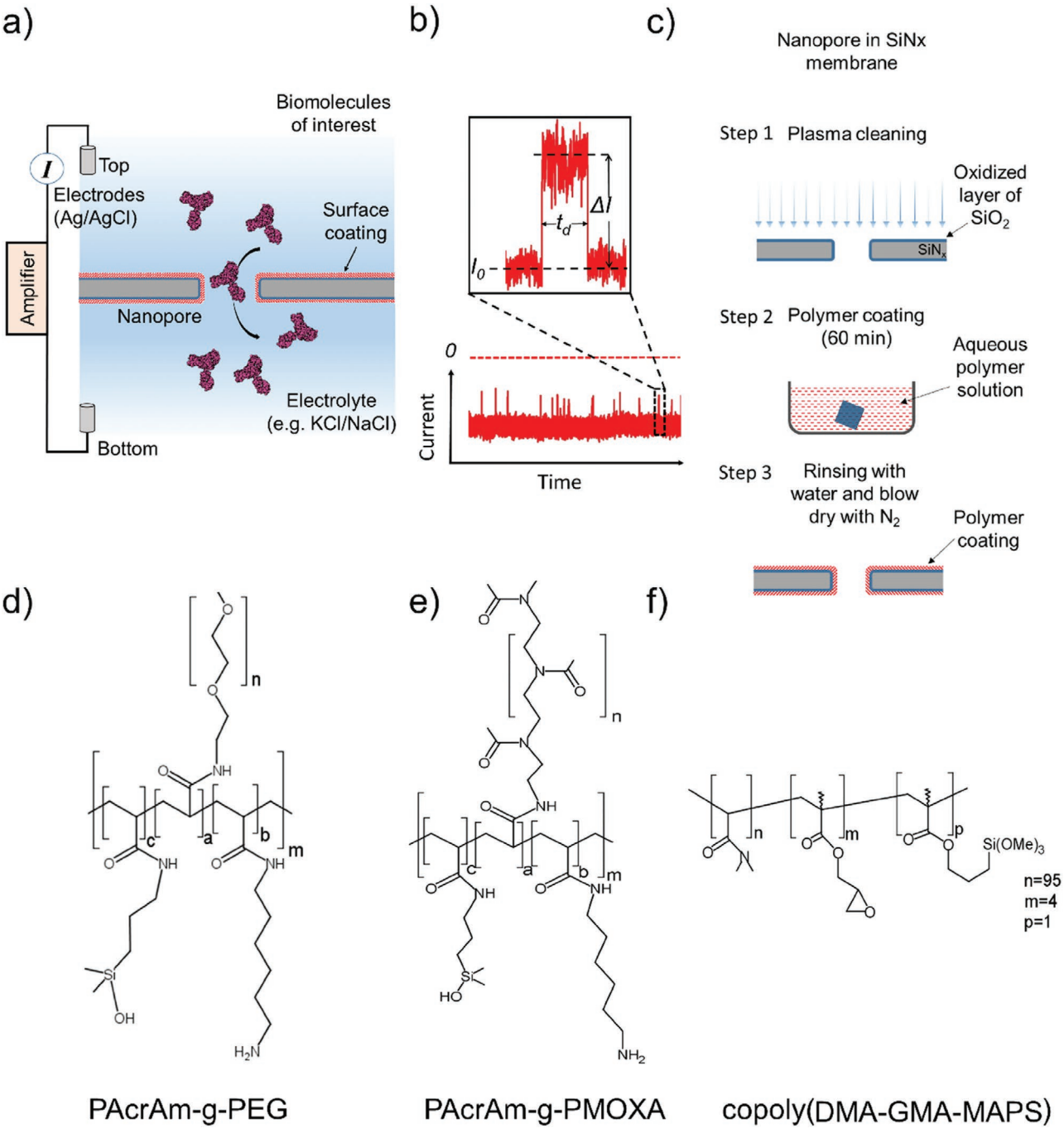

Figure 1. Schematic of the experimental nanopore setup and protocol for polymer coating. a) Nanopore setup showing a polymer-coated nanopore for resistive pulse sensing. b) Illustration of a current versus time trace with resistive pulses as a result of protein translocations through the nanopore. The inset illustrates the characteristic resistive pulse amplitude (ΔI), baseline current (I_0), and dwell time (t_d) from the translocation of a single protein. c) Schematic illustration the dip and rinse approach for coating a nanopore in a SiN_x membrane with a polymer. Chemical structures of d) PAcrAm-g-PEG, e) PAcrAm-g-PMOXA, and f) copoly(DMA-GMA-MAPS).

coating slightly decreased the noise likely by the coating-induced increase in pore resistance and concomitant decrease in thermal noise. In contrast, both PAcrAm-g-PEG and copoly(DMA-GMA-MAPS) coatings led to recordings with increased $1/f$ noise at frequencies below 1 kHz (Figure 2b,c).[49] For reference, Figure 2d shows that even the benchmark coating in our laboratory, lipid bilayer coating, led to a slight increase in low-frequency noise after coating. The change in baseline root-mean-square (rms) current noise due to polymer coating at a cutoff frequency of the low-pass filter of 50 kHz was smallest for the PAcrAm-g-PMOXA coating (decrease by 5%) and the lipid coating (increase by 7%), while the PAcrAm-g-PEG coating increased the rms noise by 15% and the copoly(DMA-GMA-MAPS) coating by 21%. The levels of baseline current noise of recordings from

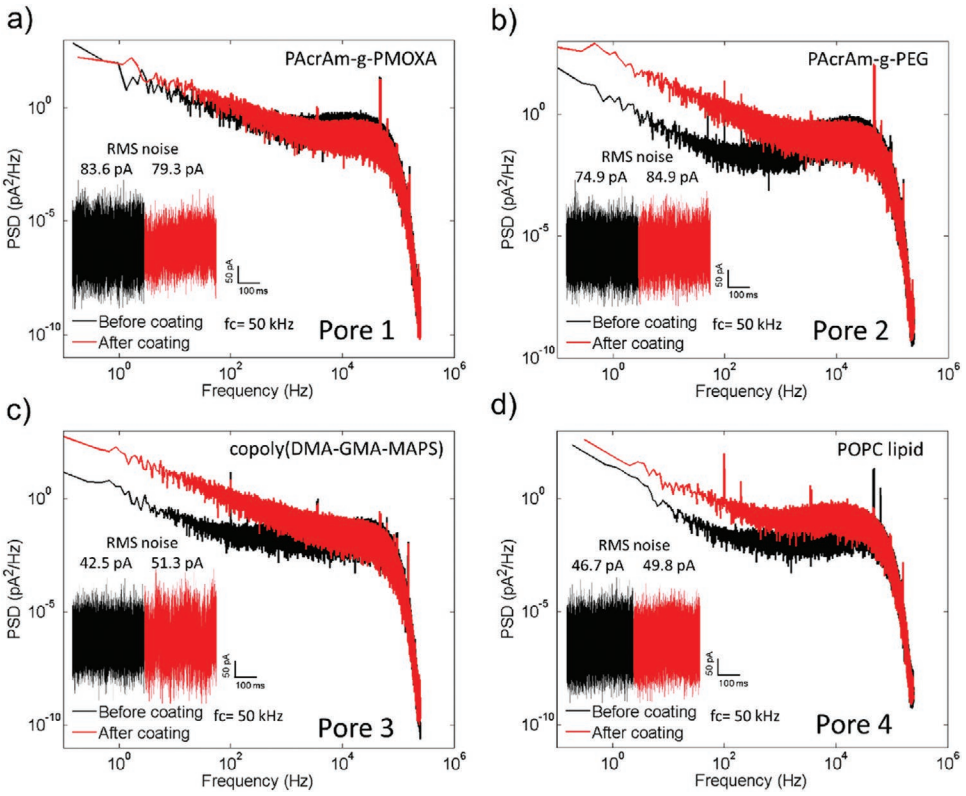

Figure 2. Power spectral density (PSD) plots obtained from 20 s recording of baseline current traces before and after polymer coating of a nanopore. a) Power spectral density for baseline current traces before and after coating nanopore with PAcrAm-g-PMOXA. The inset shows the original current traces before and after polymer coating. b) Power spectral density for baseline current traces before and after coating a nanopore with PAcrAm-g-PEG. The inset shows the original current traces before and after polymer coating. c) Power spectral density for baseline current traces before and after coating nanopore with copoly(DMA-GMA-MAPS). The inset shows the original current traces before and after polymer coating. d) Power spectra density for baseline current traces before and after coating a nanopore with POPC fluid lipid bilayer. The inset shows the original current traces before and after lipid coating.

nanopores coated with any one of the three polymer coatings were sufficiently small to resolve resistive pulses generated by proteins with sizes ranging from 50 to 150 kDa.

In order to compare the anti-adsorption properties of these polymer coatings, we carried out protein translocations. **Figure 3**a,b shows current traces for translocations of IgG through an uncoated (black) and a polymer-coated (red) nanopore, along with representative resistive pulses from each trace. In the case of uncoated pores, we observed instability in the current baseline after adding proteins. Moreover, interactions between IgG and the uncoated pore wall resulted in partial clogging of the nanopore after 5 min as indicated by an increase in resistance of pore. Nonspecific interactions between IgG and uncoated pore walls not only resulted in clogging, they also limited the rotational mobility of IgG, as shown by relatively minor current modulations within individual resistive pulses (Figure 3). In the case of polymer-coated nanopores, the current baseline remained stable at a constant level for at least one hour and resistive pulses produced by translocating IgG proteins revealed relatively large modulations in current amplitude. These modulations are consistent with previous observations with oblate-shaped proteins transiting through nanopores in the absence of surface interactions,[32,35] and are expected from theory for nonspherical objects rotating inside the electric field in the nanopore.[50]

In terms of long-term stability and benefits from these polymer coatings, we repeated at least three experiments with individual polymer-coated pores over a week and observed no significant change in the baseline current or noise (see Figure S2 in the Supporting Information). We also did not observe any detectable loss of surface coating during dry storage based on resistance measurements in the hydrated state and we did not observe growth of the diameters of polymer coated pores during recordings. This result contrasts our previous experience with solid-state nanopores, whose diameters often increased from experiment to experiment and sometimes during experiments. In addition, these coatings eliminate the need for harsh cleaning steps between experiments, a significant benefit since cleaning with Piranha solutions, for instance, can result in unwanted pore growth and surface etching of solid-state nanopores.[51,52]

To provide a quantitative comparison between these polymers for their ability to prevent protein adsorption, we determined the dwell time (t_d, i.e., the duration between a single protein entering and exiting the nanopore) and analyzed t_d distributions for hundreds to thousands individual IgG translocations through pores with and without polymer coatings (**Figure 4**). We also compared recordings using these polymer coatings to recordings using lipid bilayer coated nanopores. To do so, we use the dwell time ratio (number of resistive pulses

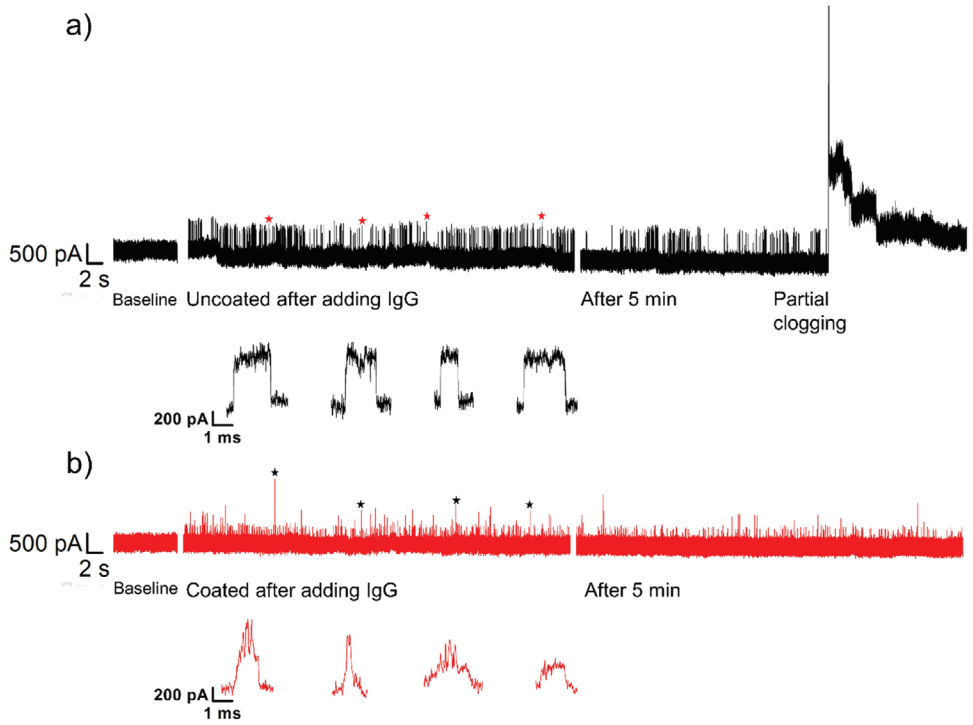

Figure 3. Comparison of resistive pulses from single-molecule translocations of IgG through an uncoated and a polymer-coated nanopore. a) Original current traces (in black) for an uncoated nanopore before (i.e., baseline trace) and after the addition of IgG at a final concentration of 400×10^{-9} M. The two 60 s traces after adding IgG presented here show the initial current trace and a trace that we recorded 5 min after protein addition. Reduction of the current through the nanopore indicates partial clogging of the uncoated nanopore. The inset show individual translocation events of IgG recorded with the uncoated nanopore. b) Current traces (in red) for polymer-coated (PAcrAm-g-PEG) nanopore before (i.e., baseline current) and after the addition of IgG at a final concentration of 400×10^{-9} M. The two 60 s traces after adding IgG presented here show the initial current trace and a trace that we recorded 5 min after protein addition. The baseline current recorded with this polymer-coated nanopore was typically stable at a constant level over long recording times (>60 min). The inset shows individual translocation events of IgG through the polymer-coated nanopore.

with t_{d10-50} devided by number of resistive pulses with $t_{d10-200}$) as explained in Note S1 in the Supporting Information and compare the experimentally determined dwell time ratio with the theoretically expected ideal ratio as estimated by the biased first passage time theory[53,54] (see Figure S1 in the Supporting Information). **Table 1** summarizes the dwell time ratios for translocation of IgG in the case of uncoated and polymer coated nanopores. Remarkably, coatings from PacrAm-g-PMOXA or copoly(DMA-GMA-MAPS) resulted in a dwell time ratio that deviated by less than 20% from the theoretically expected ratio that would be observed in the absence of any nonspecific interactions. This agreement indicates excellent nonadhesive properties of these coating during IgG translocations.[55] Table 1 also shows that these polymer coatings were approaching the performance of lipid bilayer coatings in terms of preventing nonspecific surface interactions.

Figure 5 shows that resistive pulses generated by translocations of IgG through uncoated nanopores led to overestimates of volume and to length-to-diameter ratios that were skewed toward m values of 1. In contrast, experiments with two (i.e., with PAcrAm-g-PMOXA and PAcrAm-g-PEG) of the three polymer coatings led to a good agreement of the estimates of both parameters with the expected reference values. Volume estimation of IgG was slightly smaller than reference values for experiments with nanopores coated with PAcrAm-g-PEG, while PAcrAm-g-PMOXA coated nanopores produced the best agreement for both the length-to-diameter ratio and volume with reference values and with values determined with a lipid bilayer coated nanopore. On the other hand, experiments with copoly(DMA-GMA-MAPS) coated nanopores led to overestimation of the volume of IgG and length-to-diameter ratios corresponding to slightly more pronounced oblate shapes than the expected value. We attribute inaccurate estimates of length-to-diameter ratio in experiments with uncoated nanopores to inadequate or biased sampling of those protein orientations that result in the minimum and maximum current blockade because of nonspecific interactions with the pore walls. In other words, because the IgG proteins were adsorbing to the pore walls (Figure 4a), they were unable to sample all possible orientations within the pore (Figure 5a). We hypothesize that wall interactions favor orientations with maximum contact area. Hence, the lengthwise orientation for both oblates and prolates are likely favored leading to an under-representation of ΔI_{max} and over-representation of ΔI_{min}. This effect would skew m values toward 1 as observed with uncoated pores. Moreover, in prior work,[35] we demonstrated that off-axis effects from translocations near the pore wall lead to overestimations of volume and m values biased toward 1.

In order to determine the performance of these polymer coatings for estimating the length-to-diameter ratios and volumes of several unlabeled single proteins with different shape, we carried out translocation experiments with anti-biotin Fab

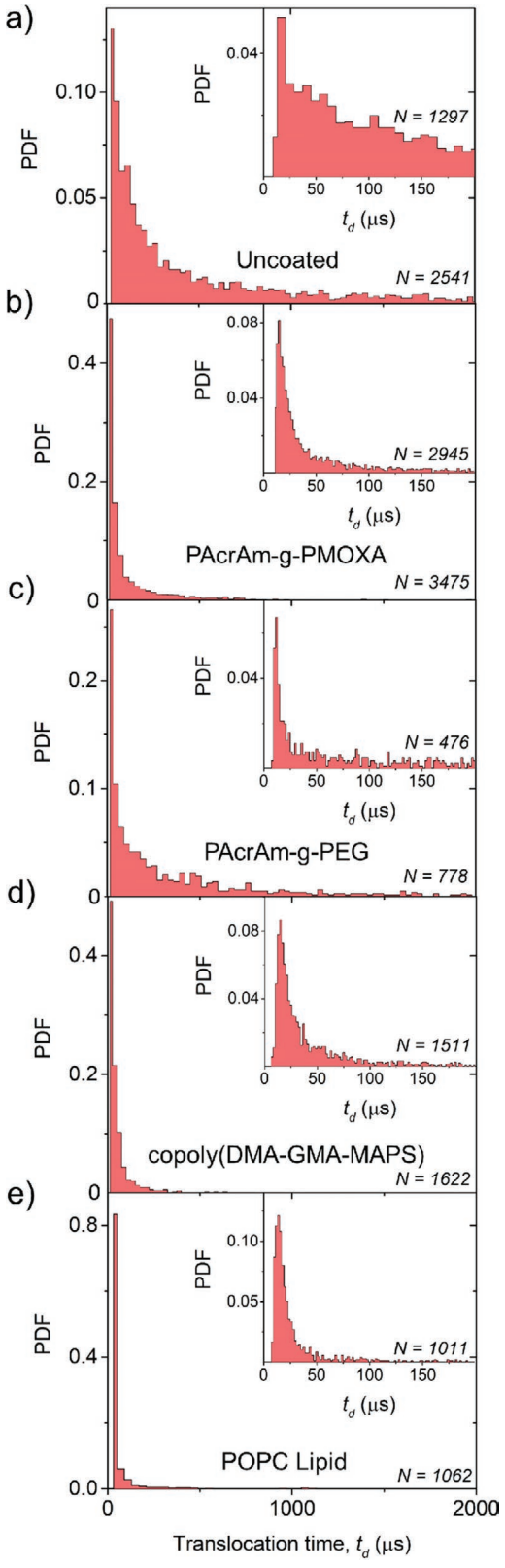

Figure 4. Comparison of dwell time (t_d) distributions from resistive pulses from the translocation of individual IgG proteins through uncoated and polymer or lipid bilayer-coated nanopores. a) Experimentally measured dwell time (t_d) distribution of IgG translocations through an uncoated nanopore. The inset shows the t_d distribution for resistive pulses with t_d values <200 μs (N = 1297, i.e. 51%). b) Dwell time (t_d) distributions of IgG translocations through nanopore coated with PAcrAm-g-PMOXA. The inset shows resistive pulses with t_d values <200 μs (N = 2945 i.e. 85%). c) Dwell time distribution of the IgG translocations through nanopore coated with PAcrAm-g-PEG. The inset shows the t_d distribution for resistive pulses with t_d value <200 μs (N = 476 i.e. 61%). d) Dwell time distribution of IgG translocations through nanopore coated with copoly(DMA-GMA-MAPS). The inset shows the t_d distribution for translocation events with t_d values <200 μs (1511 i.e. 93%). e) Dwell time distribution of IgG translocations through lipid bilayer coated nanopore. The inset shows the t_d distribution for resistive pulses with t_d values <200 μs (N = 1011 i.e. 95%). We used a bin size of 25 μs for the main figure and a the bin size of 5 μs for the insets showing resistive pulses with t_d values <200 μs.

Table 1. Comparison of the theoretically predicted ratios between the expected probability of IgG translocation events with a dwell time of 10–50 μs (t_{d10-50}) and translocation events with a dwell time of 10–200 μs ($t_{d10-200}$).

Coating	Estimates of $t_{d10-50}/t_{d10-200}$		Deviation of experimental from theoretical [%]
	Theoretical[a)]	Experimental	
Uncoated	0.96	0.37	61
PAcrAm-g-PMOXA	0.86	0.74	14
PAcrAm-g-PEG	0.86	0.58	33
copoly(DMA-GMA-MAPS)	0.94	0.78	17
POPC lipid bilayer	0.99	0.89	10

[a)]Theoretical estimates based on the biased first passage time theory using the relevant parameters for each experiment including pore length, pore diameter, charge of the protein at the pH of recording buffer, and applied voltage and diffusion coefficient inside a confinement. We assumed no electroosmotic flow.

fragment, hemoglobin (Hb), immunoglobulin (IgG), and streptavidin (SA) proteins. **Figure 6** shows results of these shape estimates for translocations through nanopores coated with PAcrAm-g-PEG and PAcrAm-g-PMOXA; these estimates agreed within ±17% with reference values (also see Table S1 in the Supporting Information). These results indicate that the estimates of volume and shape of single proteins that resulted from PAcrAm-g-PMOXA and PAcrAm-g-PEG polymer coated nanopores were almost as accurate as with the lipid bilayer coated nanopores and far superior to estimates from uncoated nanopores. We were able to use the same nanopore to carry out several experiments using different proteins such as Fab, Hb, SA, and IgG. In addition, we could use the same pore for at least three experiments within one week without detectable loss of polymer coating or change in baseline current or performance of the coated nanopore.

We previously demonstrated that fluid lipid bilayer coatings can be used to tailor surface properties and the size of nanopores.[33] While these lipid coatings provide the best performance in minimizing nonspecific surface interactions of pore walls with proteins,[32–34] we have unfortunately struggled with poor success rates (≈10%) when attempting to coat nanopores with lipid bilayers.[32] Experiments often failed because the lipids did not form a supported lipid bilayer on the walls of the nanopore or because they appeared to coat the walls in the pores unevenly resulting in a noisy and unstable baseline current after coating.[32] In addition to lipid bilayer coatings,

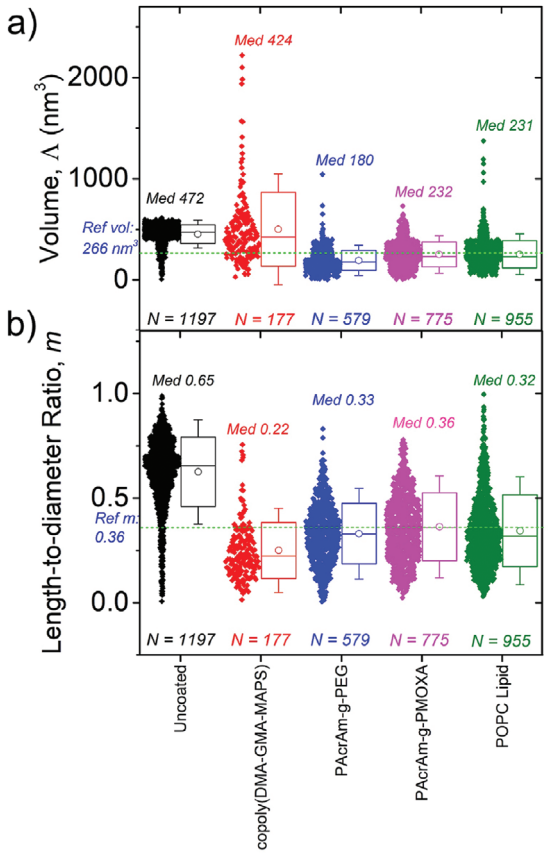

Figure 5. Comparison of volume and length-to-diameter ratio approximation of IgG as they translocated through uncoated nanopores or through pores coated with three different polymers copoly(DMA-GMA-MAPS), PAcrAm-g-PEG, and PAcrAm-g-PMOXA or with a POPC lipid bilayer. a) Volume estimates from translocation events of single IgG proteins through uncoated and coated (i.e., copoly(DMA-GMA-MAPS), PAcrAm-g-PEG, PAcrAm-g-PMOXA, and POPC lipid bilayer) nanopores. b) Estimates of the length-to-diameter ratio of single IgG proteins as determined from translocations through uncoated and coated nanopores. The diamonds show parameter estimates from single event analysis with horizontal lines in the box representing the median and quartile values. The median values ("Med") for the volume and the length-to-diameter ratio of each protein estimated using nanopore are shown. The reference values ("Ref") of length-to-diameter and volume as determined from the 3D structure of IgG obtained from the Protein Data Bank (PDB) are marked with a green dotted line. The open circles show the mean values for each data set with whiskers spanning from the 10th to the 90th percentile.

we recently also explored the possible benefits of coating nanopores with the detergent Tween-20 with regard to its ability to minimize nonspecific surface interactions.[28,35] We found that Tween-20 coated pores produced volume estimates in agreement with reference values, but length-to-diameter estimates with these pores were skewed toward m values of 0.5 as reported by Houghtaling et al.[35] As with the results from uncoated pores, a large fraction of the dwell times observed with Tween-20 coated pores lasted much longer than theoretically predicted suggesting that Tween-20 did not sufficiently reduce nonspecific interactions between the nanopore walls and proteins. Therefore, the polymer coatings presented here, especially PAcrAm-g-PMOXA and PacrAm-g-PEG, provide robust and versatile alternatives to lipid bilayers and other previously reported nonstick coatings for characterizing single proteins in solid-state nanopores.

3. Conclusion

Covalently attached polyacrylamide-based polymer surface coatings address at least four key challenges associated with label-free characterization of single proteins using solid-state nanopores. These coatings: 1) minimize nonspecific surface interactions between biomolecules and the pore walls favoring free translocation of proteins, 2) enable repeated and prolonged experiments of protein translocation without clogging and baseline shifts, 3) eliminate the need for stringent cleaning protocols of nanopores between experiments, and 4) enable estimates of volume and length-to-diameter ratio of untethered, unlabeled proteins that are in close agreement with reference values. These polymer coatings are thus well suited for a variety of protein biophysics and protein analysis applications, in particular when solution-based analyses are favorable, for instance for characterizing heterogeneous populations of natively folded, unlabeled single proteins or for interrogating dynamic assemblies of protein-protein complexes.

4. Experimental Section

Materials: TEM grids on silicon scaffolds (4 × 4 mm frame) with 30 nm thick free-standing silicon nitride windows (10 × 10 μm) were purchased from Norcada Inc., Canada. Polymers designed to minimize protein adhesion, namely, poly(acrylamide)-g-(PMOXA, 1,6-hexanediamine, 3-amino-propyldimethylsilanol) in short PAcrAm-g-PMOXA and poly(acrylamide)-g-(PEG-azide, 1,6-hexanediamine, 3-amino-propyldimethylsilanol) in short PAcrAm-g-PEG were obtained from SuSoS AG, Switzerland,[42,43,56] and a poly(dimethyl acrylamide) copolymer with glycidyl methacrylate (GMA) in short P(DMA-GMA-MAPS) was synthesized by the Istituto di Scienze e Tecnologie Chimiche (SCITEC), Italy. Antigen-binding fragment (Fab) of anti-biotin IgG (800-101-098) was purchased from Rockland Immunochemicals. Other proteins, such as antibiotin immunoglobulin G (IgG) (B3640), hemoglobin (Hb) (H7379), and streptavidin (SA) (4152800), were obtained from Sigma-Aldrich. All other chemicals and buffers were purchased from Sigma-Aldrich unless otherwise stated. The nanopores used in this work (see Table S2 in the Supporting Information) were fabricated either by drilling with helium ion milling (HIM)[57] controlled dielectric breakdown (CBD)[58,59] or ion beam sculpting.[60] Proteins were used in buffer solution with concentration in the range of (300–400) × 10^{-9} M.

Surface Coating: For the PAcrAm-g-PEG and PAcrAm-g-PMOXA polymers, chips were cleaned using oxygen plasma (Diener Nano, 90% power, O_2 atmosphere, 0.3 mbar) for 30 s on each side prior to coating. Coating solutions were prepared with a polymer concentration of 0.1 mg mL^{-1} in ultrapure water (18.2 MΩ cm) containing 10 × 10^{-3} M HEPES buffer with pH 7.4. Samples were immersed in the coating solution and incubated for 60 min at room temperature followed by rinsing the chips thoroughly with ultrapure water three times by dipping them in microwells filled with ultrapure water using a microwell plate before drying with a stream of N_2. Samples were analyzed using X-ray photoelectron spectroscopy (XPS) to confirm the presence of a surface coating by the polymer.

For the copoly(DMA-GMA-MAPS) polymer, samples were cleaned with Piranha solution (i.e., a 3:1 (v/v) freshly prepared, hot mixture of concentrated H_2SO_4 and 30% (v/v) aqueous H_2O_2) for 15 min prior to coating followed by copious rinsing with ultrapure water. Coating

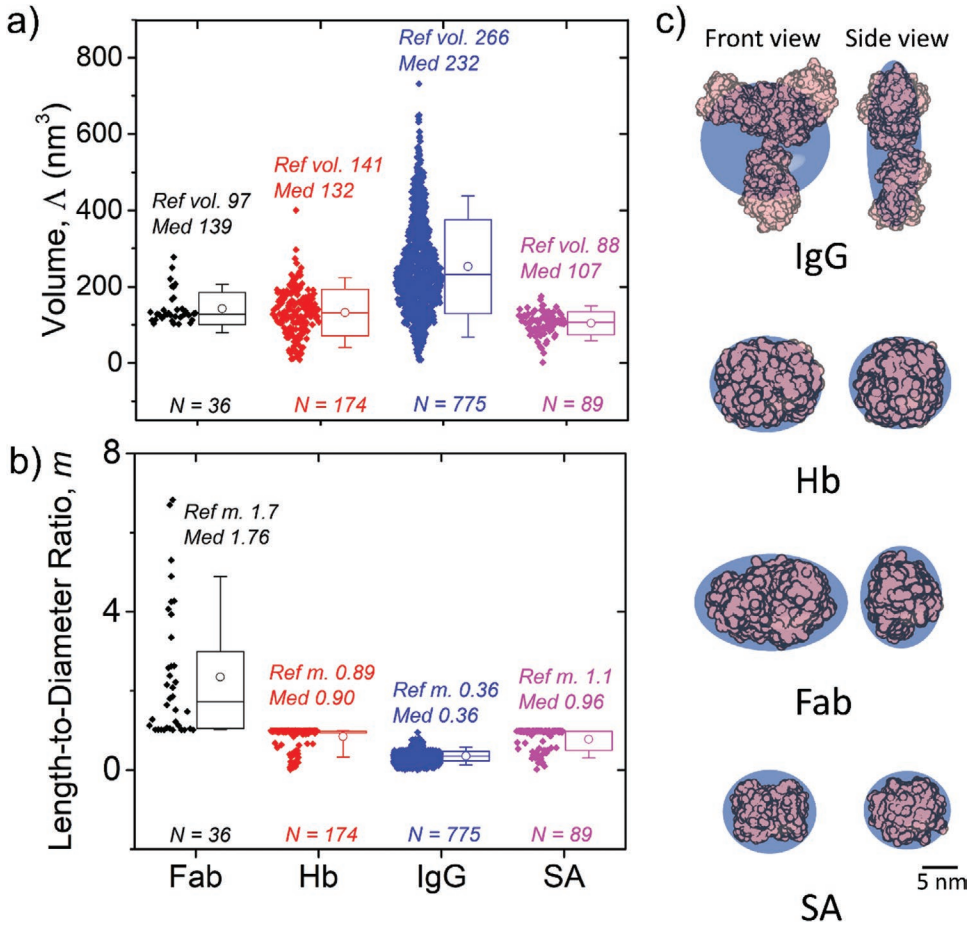

Figure 6. Volume (∧) and length-to-diameter ratio (*m*) of four different proteins with a range of ellipsoidal shapes, i.e., antigen-binding fragment (Fab), hemoglobin (Hb), immunoglobulin (IgG), and streptavidin (SA) as determined using polymer-coated nanopores and comparison of the determined values with the reference values. a) Volume approximations from single-molecule translocations of Fab, Hb, IgG, and SA proteins through PAcrAm-g-PEG and PAcrAm-g-PMOXA coated (for IgG) nanopores. b) Length-to-diameter ratio (*m*) estimates for Fab, Hb, IgG, and SA as determined using polymer-coated nanopores. Median ("Med") and reference ("Ref") values for the volume of these proteins are shown. Reference values for the length-to-diameter ratio and volume as determined from the 3D structure of these proteins obtained from PDB. The diamonds show parameter estimates from single event analysis with horizontal lines in the box representing the median and quartile values. The mean values are shown as open circles for each data set with the whiskers spanning from the 10th to the 90th percentile. c) Comparison of the approximate shape of four different proteins as determined by analysis of resistive pulses (blue spheroids) with the 3D structure from the PDB (immunoglobulin G, 1HZH; hemoglobin, 1GZX; antigen binding fragment Fab, 1F8T; and streptavidin, 3RY1).

solution of 1 mg mL^{-1} polymer concentration was prepared in ultrapure water. The chips were immersed in the coating solution and incubated for 30 min at room temperature. After incubation, they were copiously rinsed with ultrapure water followed by drying with a stream of N_2 and baking at 60 °C in an oven for 30 min followed by mounting them in PDMS scaffolds for use in resistive pulse sensing experiments.

Nanopores were coated with lipid bilayer coatings using small unilamellar vesicles (SUVs) prepared in 150 × 10^{-3} M KCl and 10 × 10^{-3} M HEPES at pH 7.4 as explained previously.[32–34] These SUVs were deposited on one side of the nanopore and incubated for 20 min to form the supported lipid bilayer followed by washing the chips by flushing the surface with copious volumes of ultrapure water.

Resistive Pulse Sensing: All resistive pulse sensing experiments were carried out as described by Yusko et al.[32] and Houghtaling et al.,[35] using a recording buffer containing 2 M KCl and 10 × 10^{-3} M HEPES (pH 7.4). Polymer-coated nanopores were allowed to hydrate and equilibrate for 15 min in the recording buffer before initiating protein translocation. Ag/AgCl pellet electrodes were used to apply potential differences of +0.1 or –0.1 V across the nanopore using an AxoPatch 200B patch-clamp amplifier (Molecular Devices) with an effective bandwidth of 57 kHz.[61] All the data were recorded at a sampling rate of 500 kHz, approximately ten times of the bandwidth of the amplifier. Resistive pulses were defined as the translocation of single protein if we observed a reduction of the absolute magnitude of the baseline current by more than five times the standard deviation of the noise.[35,53] Analyses of resistive pulses were carried out to determine the dwell time, shape, and volume using custom MATLAB (MathWorks) software. After use, the polymer-coated nanopores were rinsed with ultrapure water, dried under a flow of N_2, and then they were stored dry. To reuse these coated chips, the polymer-coated pores were again rinsed with ultrapure water, dried with a stream of N_2, and were mounted in the experimental setup using PDMS to define and contain the top and bottom liquid compartments.

For quantitative analysis of resistive pulses, we analyzed all events that were at least 10 µs long for dwell time (t_d) and we analyzed all events that were at least 150 µs for $\Delta I/I_0$ determination.[35] Volume and length-to-diameter ratios were determined by analyzing individual translocation events of proteins with dwell times between 150 and 2000 µs, as described previously.[32,35,58] The theoretical estimations of t_d distributions were carried out based on the biased first passage time

theory reported by Ling and Ling.[62] In order to estimate the diffusion coefficient of IgG protein inside the confinement of a nanopore, the diffusion coefficient of IgG in bulk water at 20 °C (3.9×10^{-7} cm^2 s^{-1}) was divided by a factor of 5 as proposed by Dix and Verkman.[63] The net charge of IgG protein at the pH of the recording buffer (pH 7.4) was $-3.6 \times e$.[32] No electroosmotic flow was assumed in the pore for this theoretical prediction of t_d distributions.

Supporting Information

Supporting Information is available from the Wiley Online Library or from the author.

Acknowledgements

This work was financially supported by the Swiss National Science Foundation (M.M., Grant No. 200021-169304) and the Adolphe Merkle Foundation, Switzerland.

Conflict of Interest

The authors declare no conflict of interest.

Keywords

free translocation, non-fouling coatings, polymer coatings, single-molecules, solid-state nanopores

Received: March 5, 2020
Revised: May 13, 2020
Published online:

[1] D. Fologea, B. Ledden, D. S. McNabb, J. Li, *Appl. Phys. Lett.* **2007**, *91*, 053901.
[2] W. Timp, G. Timp, *Sci. Adv.* **2020**, *6*, eaax8978.
[3] L. Restrepo-Pérez, C. Joo, C. Dekker, *Nat. Nanotechnol.* **2018**, *13*, 786.
[4] J. Houghtaling, J. List, M. Mayer, *Small* **2018**, *14*, 1802412.
[5] Y. Feng, Y. Zhang, C. Ying, D. Wang, C. Du, *Genomics, Proteomics Bioinf.* **2015**, *13*, 4.
[6] M. Wanunu, *Phys. Life Rev.* **2012**, *9*, 125.
[7] M. Jain, H. E. Olsen, B. Paten, M. Akeson, *Genome Biol.* **2016**, *17*, 239.
[8] D. Stoddart, A. J. Heron, E. Mikhailova, G. Maglia, H. Bayley, *Proc. Natl. Acad. Sci. USA* **2009**, *106*, 7702.
[9] C. Dekker, *Nat. Nanotechnol.* **2007**, *2*, 209.
[10] A. R. Hall, A. Scott, D. Rotem, K. K. Mehta, H. Bayley, C. Dekker, *Nat. Nanotechnol.* **2010**, *5*, 874.
[11] P. Goyal, P. V. Krasteva, N. Van Gerven, F. Gubellini, I. Van den Broeck, A. Troupiotis-Tsaïlaki, W. Jonckheere, G. Péhau-Arnaudet, J. S. Pinkner, M. R. Chapman, S. J. Hultgren, S. Howorka, R. Fronzes, H. Remaut, *Nature* **2014**, *516*, 250.
[12] L. Movileanu, S. Howorka, O. Braha, H. Bayley, *Nat. Biotechnol.* **2000**, *18*, 1091.
[13] E. A. Manrao, I. M. Derrington, A. H. Laszlo, K. W. Langford, M. K. Hopper, N. Gillgren, M. Pavlenok, M. Niederweis, J. H. Gundlach, *Nat. Biotechnol.* **2012**, *30*, 349.
[14] R. Stefureac, Y.-t. Long, H.-B. Kraatz, P. Howard, J. S. Lee, *Biochemistry* **2006**, *45*, 9172.
[15] J. J. Kasianowicz, J. W. Robertson, E. R. Chan, J. E. Reiner, V. M. Stanford, *Annu. Rev. Anal. Chem.* **2008**, *1*, 737.
[16] J. W. F. Robertson, C. G. Rodrigues, V. M. Stanford, K. A. Rubinson, O. V. Krasilnikov, J. J. Kasianowicz, *Proc. Natl. Acad. Sci. USA* **2007**, *104*, 8207.
[17] H. Bayley, P. S. Cremer, *Nature* **2001**, *413*, 226.
[18] W. Shi, A. K. Friedman, L. A. Baker, *Anal. Chem.* **2017**, *89*, 157.
[19] J. Li, M. Gershow, D. Stein, E. Brandin, J. A. Golovchenko, *Nat. Mater.* **2003**, *2*, 611.
[20] R. D. Maitra, J. Kim, W. B. Dunbar, *Electrophoresis* **2012**, *33*, 3418.
[21] N. A. W. Bell, C. R. Engst, M. Ablay, G. Divitini, C. Ducati, T. Liedl, U. F. Keyser, *Nano Lett.* **2012**, *12*, 512.
[22] K. Lee, K.-B. Park, H.-J. Kim, J.-S. Yu, H. Chae, H.-M. Kim, K.-B. Kim, *Adv. Mater.* **2018**, *30*, 1704680.
[23] V. Hlady, J. Buijs, *Curr. Opin. Biotechnol.* **1996**, *7*, 72.
[24] M. Firnkes, D. Pedone, J. Knezevic, M. Döblinger, U. Rant, *Nano Lett.* **2010**, *10*, 2162.
[25] E. C. Yusko, R. An, M. Mayer, *ACS Nano* **2010**, *4*, 477.
[26] P. Chen, T. Mitsui, D. B. Farmer, J. Golovchenko, R. G. Gordon, D. Branton, *Nano Lett.* **2004**, *4*, 1333.
[27] Y. Xie, J. Xue, L. Wang, X. Wang, K. Jin, L. Chen, Y. Wang, *Langmuir* **2009**, *25*, 8870.
[28] X. Li, R. Hu, J. Li, X. Tong, J. J. Diao, D. Yu, Q. Zhao, *Appl. Phys. Lett.* **2016**, *109*, 143105.
[29] Z. Tang, B. Lu, Q. Zhao, J. Wang, K. Luo, D. Yu, *Small* **2014**, *10*, 4332.
[30] B. N. Anderson, M. Muthukumar, A. Meller, *ACS Nano* **2013**, *7*, 1408.
[31] S. Zhang, G. Liu, H. Chai, Y.-D. Zhao, L. Yu, W. Chen, *Electrochem. Commun.* **2019**, *99*, 71.
[32] E. C. Yusko, B. R. Bruhn, O. M. Eggenberger, J. Houghtaling, R. C. Rollings, N. C. Walsh, S. Nandivada, M. Pindrus, A. R. Hall, D. Sept, J. Li, D. S. Kalonia, M. Mayer, *Nat. Nanotechnol.* **2017**, *12*, 360.
[33] E. C. Yusko, J. M. Johnson, S. Majd, P. Prangkio, R. C. Rollings, J. Li, J. Yang, M. Mayer, *Nat. Nanotechnol.* **2011**, *6*, 253.
[34] O. M. Eggenberger, G. Leriche, T. Koyanagi, C. Ying, J. Houghtaling, T. B. H. Schroeder, J. Yang, J. Li, A. Hall, M. Mayer, *Nanotechnology* **2019**, *30*, 325504.
[35] J. Houghtaling, C. Ying, O. M. Eggenberger, A. Fennouri, S. Nandivada, M. Acharjee, J. Li, A. R. Hall, M. Mayer, *ACS Nano* **2019**, *13*, 5231.
[36] G. F. Schneider, Q. Xu, S. Hage, S. Luik, J. N. H. Spoor, S. Malladi, H. Zandbergen, C. Dekker, *Nat. Commun.* **2013**, *4*, 2619.
[37] M. Wanunu, A. Meller, *Nano Lett.* **2007**, *7*, 1580.
[38] O. M. Eggenberger, C. Ying, M. Mayer, *Nanoscale* **2019**, *11*, 19636.
[39] G. Emilsson, Y. Sakiyama, B. Malekian, K. Xiong, Z. Adali-Kaya, R. Y Lim, A. B. Dahlin, *ACS Cent. Sci.* **2018**, *4*, 1007.
[40] J. Roman, O. Français, N. Jarroux, G. Patriarche, J. Pelta, L. Bacri, B. Le Pioufle, *ACS Sens.* **2018**, *3*, 2129.
[41] J. Roman, N. Jarroux, G. Patriarche, O. Français, J. Pelta, B. Le Pioufle, L. Bacri, *ACS Appl. Mater. Interfaces* **2017**, *9*, 41634.
[42] S. Weydert, S. Zurcher, S. Tanner, N. Zhang, R. Ritter, T. Peter, M. J. Aebersold, G. Thompson-Steckel, C. Forro, M. Rottmar, F. Stauffer, I. A. Valassina, G. Morgese, E. M. Benetti, S. Tosatti, J. Voros, *Langmuir* **2017**, *33*, 8594.
[43] M. Aramesh, C. Forró, L. Dorwling-Carter, I. Lüchtefeld, T. Schlotter, S. J. Ihle, I. Shorubalko, V. Hosseini, D. Momotenko, T. Zambelli, E. Klotzsch, J. Vörös, *Nat. Nanotechnol.* **2019**, *14*, 791.
[44] C. Zilio, L. Sola, F. Damin, L. Faggioni, M. Chiari, *Biomed. Microdevices* **2014**, *16*, 107.
[45] T. Z. Butler, J. H. Gundlach, M. A. Troll, *Biophys. J.* **2006**, *90*, 190.
[46] A. Meller, L. Nivon, E. Brandin, J. Golovchenko, D. Branton, *Proc. Natl. Acad. Sci. USA* **2000**, *97*, 1079.

[47] E. C. Yusko, P. Prangkio, D. Sept, R. C. Rollings, J. Li, M. Mayer, *ACS Nano* **2012**, *6*, 5909.
[48] Â. Serrano, S. Zürcher, S. Tosatti, N. D. Spencer, *Macromol. Rapid Commun.* **2016**, *37*, 622.
[49] R. M. M. Smeets, U. F. Keyser, N. H. Dekker, C. Dekker, *Proc. Natl. Acad. Sci. USA* **2008**, *105*, 417.
[50] D. C. Golibersuch, *Biophys. J.* **1973**, *13*, 265.
[51] E. Laarz, B. V. Zhmud, L. Bergström, *J. Am. Ceram. Soc.* **2000**, *83*, 2394.
[52] B. V. Zhmud, L. Bergström, *J. Colloid Interface Sci.* **1999**, *218*, 582.
[53] D. Pedone, M. Firnkes, U. Rant, *Anal. Chem.* **2009**, *81*, 9689.
[54] C. Plesa, S. W. Kowalczyk, R. Zinsmeester, A. Y. Grosberg, Y. Rabin, C. Dekker, *Nano Lett.* **2013**, *13*, 658.
[55] D. J. Niedzwiecki, J. Grazul, L. Movileanu, *J. Am. Chem. Soc.* **2010**, *132*, 10816.
[56] R. Konradi, B. Pidhatika, A. Mühlebach, M. Textor, *Langmuir* **2008**, *24*, 613.
[57] I. Shorubalko, L. Pillatsch, I. Utke, *Helium Ion Microscopy*, Springer, Berlin **2016**, p. 355.
[58] C. Ying, J. Houghtaling, O. M. Eggenberger, A. Guha, P. Nirmalraj, S. Awasthi, J. Tian, M. Mayer, *ACS Nano* **2018**, *12*, 11458.
[59] H. Kwok, K. Briggs, V. Tabard-Cossa, *PLoS One* **2014**, *9*, e92880.
[60] J. Li, D. Stein, C. McMullan, D. Branton, M. J. Aziz, J. A. Golovchenko, *Nature* **2001**, *412*, 166.
[61] J. D. Uram, K. Ke, M. Mayer, *ACS Nano* **2008**, *2*, 857
[62] D. Y. Ling, X. S. Ling, *J. Phys.: Condens. Matter* **2013**, *25*, 375102.
[63] J. A. Dix, A. S. Verkman, *Annu. Rev. Biophys.* **2008**, *37*, 247.